https://doi.org/10.5194/bg-2020-477
Preprint. Discussion started: 11 January 2021

Biogeosciences Discussions

Spatial and temporal variability of pCO_2 and CO_2 emissions from the Dongjiang River in South China

Boyi Liu[1], Mingyang Tian[2], Kaimin Shih[3], Chun Ngai Chan[1], Xiankun Yang[4], Lishan Ran[1]

[1]Department of Geography, the University of Hong Kong, Hong Kong SAR, China
[2]Institute for Geology, Center for Earth System Research and Sustainability (CEN), Universität Hamburg, Hamburg, Germany
[3]Department of Civil Engineering, the University of Hong Kong, Hong Kong SAR, China
[4]School of Geographical Sciences, Guangzhou University, Guangzhou,510006, China

Correspondence to: Lishan Ran (lsran@hku.hk)

Abstract. CO_2 efflux at the water–air interface is an essential component of the riverine carbon cycle. However, the lack of spatially resolved CO_2 emission measurement still hinges the accuracy of estimates on global riverine CO_2 emissions. By deploying floating chambers, seasonal changes in river water CO_2 partial pressure (pCO_2) and CO_2 evasion from the Dongjiang River in South China were investigated. Lateral soil CO_2 input and dilution effect caused by precipitation played critical roles in controlling riverine pCO_2 in small rivers, while the decomposition of allochthonous organic carbon is responsible for pCO_2 variability in large rivers. Temperature-normalized gas transfer velocity (k_{600}) in small rivers were 8.29 ± 11.29 m d^{-1} and 4.90 ± 3.82 m d^{-1} for the wet season and dry season, respectively, which were nearly 70 % higher than that of large rivers (3.90 ± 5.55 m d^{-1} during the wet season and 2.25 ± 1.61 m d^{-1} during the dry season). A significant correlation was observed between k_{600} and flow velocity but not wind speed regardless of river size. Majority of the surveyed rivers were net CO_2 source, exhibiting substantial seasonal variations. The mean CO_2 flux was 300.1 and 264.2 mmol m^{-2} d^{-1} during the wet season for large and small rivers, respectively, 2-fold larger than that during the dry season. The absence of commonly observed higher CO_2 fluxes in small rivers could be associated with the depletion effect caused by abundant and consistent precipitation in this subtropical monsoon catchment.

https://doi.org/10.5194/bg-2020-477
Preprint. Discussion started: 11 January 2021


Biogeosciences Discussions Open Access EGU

1 Introduction

River networks act as a processor that transfers and emits the carbon entering the water, rather than just a passive pipe that transports carbon from the terrestrial ecosystem to the ocean (Cole et al., 2007; Battin et al., 2009; Drake et al., 2018). CO_2 emissions at the water–air interface are an essential component of the riverine carbon cycle. CO_2 emitted from inland waters to the atmosphere reaches up to 2.9 PgC yr^{-1}, surpassing that transported from land to ocean through rivers (Sawakuchi et al., 2017; Drake et al., 2018). Understanding the role that rivers play in the global carbon cycle is still hindered by uncertainty on the estimate of CO_2 flux outgassing from rivers (Cole et al., 2007; Raymond et al., 2013; Sawakuchi et al., 2017; Drake et al., 2018). Riverine carbon emissions have significant temporal and spatial variations, making it challenging to quantify carbon emissions accurately. In addition, watershed geomorphology, hydrological conditions, climate, and other environmental factors can affect the CO_2 efflux in rivers (Alin et al., 2011; Abril et al., 2014; Almeida et al., 2017; Ran et al., 2017a; Borges et al., 2018). Thus, there are substantial differences in CO_2 efflux among rivers in different climate regions, or the same river but between different seasons (Denfeld et al., 2013; Rasera et al., 2013). An enhanced understanding of the temporal and spatial characteristics of the water–air CO_2 flux will facilitate a more robust estimate. However, global riverine carbon emission estimates were largely based on data disproportionately focusing on temperate and boreal regions, including North America and Europe (Raymond et al., 2013; Lauerwald et al., 2015; Drake et al., 2018). In light of this data gap, more studies are required in other data-poor regions to achieve a more accurate estimate.

Rivers in tropical and subtropical regions of East Asia and Southeast Asia are among those underrepresented regions that need more attention since they are essential participants in riverine carbon transport (Ran et al., 2015; Ran et al., 2017b; Drake et al., 2018). The high temperature in this region facilitated a high net primary productivity in the terrestrial ecosystem and intense biochemical activities, and both contributed to the carbon input dynamic from soil to rivers (Li et al., 2018). Meanwhile, rivers in this region are under the heavy influence of monsoon, and riverine CO_2 emissions vary significantly among seasons due to the changes in temperature and precipitation. In addition, different rivers in this region may have contrasting trends in CO_2 dynamic due to different underlying controlling factors. Some rivers have the highest CO_2 efflux in the wet season, while others have the highest CO_2 efflux in the dry season (Li et al., 2013; Le et al., 2018; Luo et al., 2019; Ni et al., 2019), suggesting that an increase in wet season runoff can have two distinct consequences. One possibility is

https://doi.org/10.5194/bg-2020-477
Preprint. Discussion started: 11 January 2021

that it increases external carbon inputs and CO_2 emissions (Hope et al., 2004; Johnson et al., 2008), while the other is that it leads to a dilution of CO_2 in rivers and accordingly a reduction in CO_2 emissions (Ran et al., 2017b; Li et al., 2018). Since starkly different outcomes can occur, it is important to investigate the processes behind such diverse response of rivers to the monsoon.

The Dongjiang River (DJR), located in the subtropical region of South China, is one of the three tributaries of the Pearl River. Previous studies on riverine carbon transportation and emissions in the Pearl rivers mainly focused on the Xijiang River, which was characterized by widely distributed carbonate rocks, and the estuary area of the Pearl River Delta (Yao et al., 2007; Zhang et al., 2015; Zhang et al., 2019; Liang et al., 2020). Though some studies have been conducted in the Dongjiang River basin (DJRB) focusing on carbon transport and the carbon sink effect of chemical weathering (Tao et al., 2011; Fu et al., 2014), there is still a lack of understanding of the characteristics of catchment-wide CO_2 emissions in DJRB. Furthermore, a predominantly hilly landscape combined with abundant precipitation favors the formation of a great number of small rivers in DJRB (Ding et al., 2015). However, the current estimate of basin-wide CO_2 emission from the river network was mostly based on the data from large rivers, and small rivers are heavily underrepresented (Raymond et al., 2013; Drake et al., 2018). Because the controlling factors and the input of carbon could be significantly different between large and small rivers(Johnson et al., 2008; Dinsmore et al., 2013; Hotchkiss et al., 2015; Marx et al., 2017), which can lead to very distinctive pattern of carbon dioxide evasion, More comprehensive quantification of CO_2 evasion from small headwater streams is necessary. Therefore, studies on the characteristics of riverine CO_2 emission in DJRB should be conducted among river size spectrums, and the impact of monsoon ought to be considered.

By using directly measured river water CO_2 partial pressure (pCO_2) and CO_2 efflux data from DJRB, and in conjunction with hydrological and physicochemical data, the objectives of this study were to 1) investigate the spatial and temporal pattern of pCO_2 and CO_2 emission along stream size spectrum, 2) examine the differences in hydrological and physicochemical controls of pCO_2 and the CO_2 evasion between small headwater streams and large rivers. The results of this study could shed light on the underlying controls of the spatial and temporal distribution of riverine pCO_2 and support a refined estimate of regional and global carbon budgets.

https://doi.org/10.5194/bg-2020-477
Preprint. Discussion started: 11 January 2021

2 Material and methods

2.1 Site Description

The DJR in South China is one of the three major tributaries of the Pearl River system (Figure 1). It has a 562 km long mainstem channel and a drainage area of 35,340 km^2 (Chen et al., 2011). Due to its subtropical monsoon climate, precipitation in DJRB exhibits significant seasonal variability (Figure 2a). The multi-annual average precipitation is about 1800 mm, 80 % of which is concentrated during the wet season from April to September. The Boluo Hydrological Gauge is the lowermost gauge of the Dongjiang River mainstem channel, controlling a drainage area of ~23,000 km^2. The multi-annual average water discharge at Boluo Hydrological Gauge is 23.7 km^3 (Zhang et al., 2008). About 80–90 % of this discharge is transported during the wet season (Figure 2b). The dominant land use of the catchment is forest, and the landscape is characterized by plains and hills, accounting for 87.3 % of the river basin area (Ding et al., 2015).

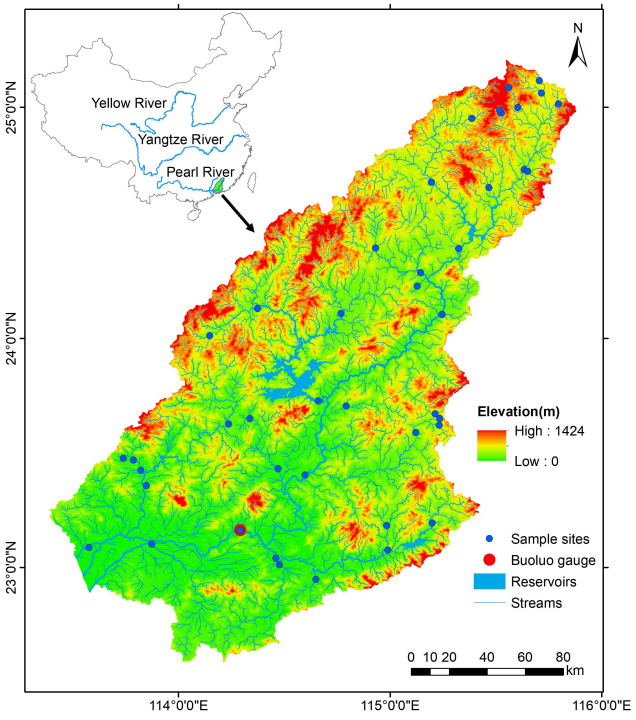

Figure 1 Location map of the Dongjiang River Basin, sampling sites, and Boluo Gauge.

https://doi.org/10.5194/bg-2020-477
Preprint. Discussion started: 11 January 2021

100

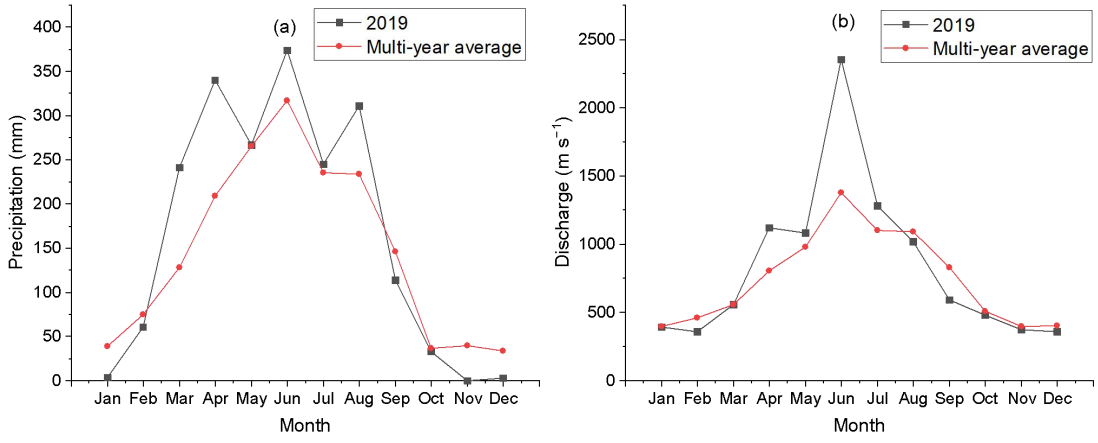

Figure 2 Monthly variations in (a) precipitation of the DJRB and (b) water discharge at the Boluo hydrological gauge, based on data provided by the Hydrological Bureau of Guangdong Province.

2.2 Field Measurement and Analysis

105 In total, there were 43 sampling sites from seven Strahler stream orders. Fourth to seven order streams were mainstem and major tributaries, while first to third order streams were small tributaries. River widths were measured by a laser rangefinder. Sampled rivers were categorized, according to their stream orders, into small rivers (first to third order streams, SR) and large rivers (fourth to seventh order streams, LR). The small rivers had an average width of 15.4 ± 10.2 m (4.8 ± 2.3 m, 10.4 ± 5.6 m,
110 22.9 ± 8.1 m for first to third order streams, respectively), while large rivers have an average width of 180.8±156.0 m (75.2 ± 51.0 m, 168.0 ± 48.6 m, 235.7 ± 29.6 m, 433.4 ± 178.0 m for fourth to seventh order streams, respectively).

In order to investigate CO_2 emissions during different hydrological conditions, we performed five fieldwork campaigns from December 2018 to October 2019, including late December 2018 to early
115 January 2019 (middle dry season), April (early wet season), early July (middle wet season), late August (late wet season) and late October 2019 (early dry season). During the field trips, water temperature, pH, and dissolved oxygen (DO) were measured with a portable multiparameter probe (Multi 3430, WTW GmbH, Germany). The pH probe was calibrated before each field trip with standard pH buffers (4.01 and 7.00). Measurements were conducted 10 cm below the water surface. To evaluate the

https://doi.org/10.5194/bg-2020-477
Preprint. Discussion started: 11 January 2021

120 contribution of metabolism on DO changes, ΔCO_2 and ΔO_2 were calculated as described by Stets et al. (2017) using:

$$\Delta CO_2 = CO_{2w} - CO_{2a} \quad (1)$$

and

$$\Delta O_2 = O_{2w} - O_{2a} \quad (2)$$

125 Where CO_{2w} and O_{2w} are measured concentrations of CO_2 and O_2 in water sample, while CO_{2a} and O_{2a} are the equilibrium CO_2 and O_2 concentrations (μmol L^{-1}).

Flow velocity was determined using a flow meter, while wind speed at 1.5 m above the water surface was measured with a Kestrel 2500 handheld anemometer and normalized to a height of 10 m (U10) using the equation from Alin et al. (2011). As the flow velocity was measured near the riverbanks, an
130 underestimation of the flow velocity is possible.

We also collected water for analyzing total alkalinity (TA) and dissolved organic carbon (DOC). Firstly, 100 ml of water samples were filtered through a pre-combusted glass fiber filter (pore size: 0.47 μm, Whatman GF/F, GE Healthcare Life Sciences, USA). Then, 50 ml of water used for TA analysis was titrated with 0.1 mol L^{-1} HCl at the same day of sampling. The remaining 50 ml of water for DOC
135 analysis was poisoned with concentrated H_2SO_4 to pH < 2 and preserved in a cooler with ice bags before analysis. DOC was determined by the high-temperature combustion method using a TOC Analyzer (Elementar Analysensysteme GmbH, Langenselbold, Germany) that has a precision better than 3 %.

2.3 Calculation of pCO_2 and CO_2 emission flux

140 The surface water pCO_2 was determined using the headspace equilibrium method, which could avoid the possible overestimation of using TA and pH to calculate pCO_2 in rivers with a relatively low pH (Abril et al., 2015). We used a 625 mL reagent bottle to collect 400 mL of water from ~10 cm below the surface, leaving 225 mL of space filled with ambient air as headspace. The bottle was then immediately capped and shaken vigorously for 1 min to achieve an equilibrium between the water and
145 the CO_2 in the headspace. Then, the bottle was connected to the calibrated Li-850 CO_2/H_2O gas analyzer (Li-Cor, Inc, USA), and the equilibrated gas in this closed loop was measured. The ambient

https://doi.org/10.5194/bg-2020-477
Preprint. Discussion started: 11 January 2021

air pCO_2 (pCO_2^{air}) was measured before the chamber deployments and varied between 380 and 450 μatm. The measurements at each site were repeated three times, and the average was then calculated. The original surface water pCO_2 ($pCO_2^{water,i}$) was finally calculated by using solubility constants (K_0) for CO_2 from Weiss (1974), Carbonate constants (K_1, K_2) from (Millero et al., 2006), and the volume of the flask, headspace, and residual system (line and gas analyzer) (Dickson et al., 2007; Ran et al., 2017a; Tian et al., 2019) using:

$$pCO_2^{water,i} = pCO_2^{headspcae,f} + (\frac{Vh+Vr}{Vw})(pCO_2^{h+r} - pCO_2^{headspcae,i})/[RTK_0(1+\frac{K_1}{[H+]}+\frac{K_1K_2}{[H+]^2})] \quad (3)$$

Where V_h, V_r and V_w, are the headspace volume, residence system volume, and water volume, respectively. R is the universal gas constant (8.314 J mol^{-1} K^{-1}), T is the water temperature in Kelvin (K), and $[H^+]$ is the concentration of hydrogen ion. $pCO_2^{headspcae,i}$ and $pCO_2^{headspace,f}$ are pCO_2 before and after the headspace equilibration, respectively. pCO_2^{h+r} is the pCO_2 of the mixed gas in the headspace and residual system during the measurement. the $pCO_2^{headspcae,i}$ was taken as the pCO_2 in ambient air before the measurement, while $pCO_2^{headspace,f}$ was calculated using:

$$pCO_2^{headspace,f} = pCO_2^{h+r} + (\frac{V_r}{V_h})(pCO_2^{h+r} - pCO_2^{headspcae,i}) \quad (4)$$

For measuring V_r, We filled the headspace with gas, which had a known pCO_2, and measured the pCO_2 in the closed loop. V_r was then estimated according to equation (2).

To reduce the artificial turbulence induced by anchored chambers, we used a small unmanned boat in the measurement, which allowed us to deploy drifting chambers freely in rivers deeper than 0.2 m and with a high flow velocity up to 2 m s^{-1}. During the deployment, CO_2 emission was determined using a circular, 8.5 L floating chamber with a water surface area of 0.113 m^2. The chamber walls were lowered about 2 cm into the water and mounted with a pneumatic rubber tire. The chamber was connected to an infrared Li-850 CO_2/H_2O gas analyzer (Li-Cor, Inc, USA) in a floating storage box through Polyurethane tubes for CO_2 analysis. An unmanned boat connected to both the chamber and box with ropes was used to deploy them near the central line of the river. Once the entire setup reached its designated location, the readings on the Li-850 were recorded at 0.5 s intervals. During the entire measurement process, the box drifted freely with the current. The Li-850 was calibrated by the

https://doi.org/10.5194/bg-2020-477
Preprint. Discussion started: 11 January 2021

manufacturer before field trips. The rate of CO_2 efflux (FCO_2 in mmol m^{-2} d^{-1}) was calculated from the observed change rate of the mole fraction S (ppm s^{-1}) using:

$$FCO_2 = (S \cdot V/A) \cdot t_1 \cdot t_2 \quad (5)$$

Where S is the slope of CO_2 accumulation in the chamber (µatm s^{-1}), V is chamber gas volume (m^3), A is the chamber area (m^2), $t_1 = 8.64 \cdot 10^4$ s d^{-1} is the conversion factor from seconds to days, and t_2 is a conversion factor from mole fraction (ppm) to concentration (mmol m^{-3}) at in situ temperature (T in K) and atmospheric pressure (p in Pa), according to the ideal gas law:

$$t_2 = p/(8.31 JK^{-1}\text{mole}^{-1} \cdot \text{T}) \cdot 1000 \quad (6)$$

The gas transfer velocity (k) was calculated from FCO_2 and pCO_2 in both water and ambient air using:

$$k = FCO_2/(K_0 \cdot (pCO_2^{water,i} - pCO_2^{air}) \quad (7)$$

To compare gas transfer velocity values among different sites, k was standardized to k_{600} as described by Alin et al. (2011) using:

$$k_{600} = k(600/Sc)^{-0.5} \quad (8)$$

Where, Sc is the Schmidt number, which is dependent on temperature (T) in degree Celsius (Wanninkhof, 1992):

$$Sc = 1911.1 - 118.11T + 3.4527T^2 - 0.4132T^3 \quad (9)$$

In total, 196 chamber measurements were made. In 19 out of 215 sample sites, the drifting chamber was unable to deploy due to shallow water or high flow velocity. Meanwhile, 8 out of 196 k_{600} data with the air−water pCO_2 gradient less than 200 µatm were also excluded, as the error in these calculations could be considerable. (Borges et al., 2004).

3 Result

3.1 Physical and Biochemical Characteristics

The Dongjiang River was characterized by substantial seasonal variations in hydrologic regimes (Table 1). Stream width in the wet season was 17.0 % and 4.6 % larger than that in the dry season for small

https://doi.org/10.5194/bg-2020-477
Preprint. Discussion started: 11 January 2021

and large rivers, respectively. The Q ranged 5 orders of magnitude from 0.01 m^3 s^{-1} in the small headwater streams during the dry season to 6690 m^3 s^{-1} in the main stem during the wet season. Water temperature was higher in July and August (21.4–33 and 21–33.4 ℃, respectively) than that in January (8.1–22.2 ℃), April (16.5–26.9 ℃), and October (17.4–29.7 ℃). pH varied from 6.38 to 8.14, with a mean of 7.08. There was no significant (independent sample t test, $p > 0.05$) change in pH between wet and dry seasons. U10 based on all stream sites was higher in large rivers (0.86 ± 0.91 and 1.43 ± 1.58 m s^{-1} in wet and dry season, respectively) than in small rivers (0.62 ± 0.61 and 0.76 ± 0.73 m s^{-1} in wet and dry season, respectively).

The streams presented low alkalinity ranging from 225 to 3025 μmol L^{-1}. Overall, lower alkalinity was observed in wet season than in dry season. In small rivers, the alkalinity in wet season (656 ± 265 μmol L^{-1}) was 21.1 % lower than the dry season (831 ± 460 μmol L^{-1}), and the lowest alkalinity was observed in April (615 ± 262 μmol L^{-1}), which was 30.4 % lower than in January (883 ± 548 μmol L^{-1}). Similarly, the alkalinity in large rivers was 790 ± 402 μmol L^{-1} in wet season, 14.5 % lower than 924 ± 411 μmol L^{-1} in dry season. However, the lowest value of alkalinity in large rivers was observed in August (739 ± 312 μmol L^{-1}) instead of April in small rivers.

Spatial and seasonal changes in DOC concentration were also observed in the surveyed rivers. DOC concentration in larges rivers (1.94 ± 1.52 mg L^{-1}) was 41.6 % higher than that in small rivers (1.37 ± 0.72 mg L^{-1}). Meanwhile, DOC concentrations in the wet season were 2.22 ± 1.82 mg L^{-1} and 1.54 ± 0.72 mg L^{-1} for large and small rivers, respectively, which were 45.1 % and 54 % higher than that in the dry season (1.53 ± 0.72 and 1.11 ± 0.63 mg L^{-1} for large and small rivers, respectively).

https://doi.org/10.5194/bg-2020-477
Preprint. Discussion started: 11 January 2021

Table 1 Seasonal Variations of Physical and Biochemical Characteristics, expressed as Mean ± SD.

Stream size	Season	Month	Water Temperature (°C)	pH	Alkalinity (μmol L^{-1})	DOC (mg L^{-1})
small	Dry	January	14.3 ± 4.1	7.05 ± 0.31	883 ± 548	1.07 ± 0.37
	Wet	April	19.9 ± 1.9	7.19 ± 0.26	615 ± 262	1.51 ± 0.58
	Wet	July	25.7 ± 2.3	7.17 ± 0.27	676 ± 227	1.59 ± 0.97
	Wet	August	27.1 ± 3.0	7.13 ± 0.38	678 ± 308	1.51 ± 0.56
	Dry	October	21.5 ± 2.6	7.08 ± 0.23	778 ± 358	1.16 ± 0.82
large	Dry	January	16.9 ± 5.5	7.00 ± 0.27	961 ± 409	1.70 ± 1.52
	Wet	April	22.1 ± 3.7	7.20 ± 0.27	890 ± 386	2.22 ± 1.65
	Wet	July	27.8 ± 2.9	6.92 ± 0.25	740 ± 305	1.97 ± 1.77
	Wet	August	28.9 ± 3.3	6.92 ± 0.26	739 ± 312	2.47 ± 2.04
	Dry	October	25.2 ± 3.1	7.13 ± 0.29	887 ± 331	1.37 ± 0.67

3.2 Spatial and Seasonal variation in pCO_2

The pCO_2 ranged from 15 to 6323 μatm with a catchment-wide average of 1748 μatm and showed considerable temporal and spatial variation throughout the sampling period. There was an increasing trend of observed pCO_2 from small to large rivers. On average, the pCO_2 values were 856 ± 444, 1481 ± 979, 1354 ± 753, 2332 ± 1330, 2142 ± 1016, 2271 ± 1121, and 2168 ± 1046 μatm for streams from first to seventh order, respectively (Figure 3a). The stronger increase in pCO_2 occurred between third and fourth order streams (from 1354 ± 753 to 2332 ± 1330 μatm). Overall, pCO_2 in large rivers (2250 ± 1178 μatm) was 76.3 % higher than that in small rivers (1276 ± 796 μatm).

Seasonal variations of pCO_2 differ across the stream size spectrum (Figure 3b). In small rivers, the highest pCO_2 was observed in April (1506 ± 880 μatm), which was 50.3 % higher compared to January (1002 ± 660 μatm). pCO_2 then decreased in July (1131 ± 589 μatm) and increased in August (1325 ± 863 μatm) and October (1414 ± 900 μatm). Compared to small rivers, the peak of pCO_2 in large rivers occurred later but persisted for a longer period of time. In large rivers, an increase in pCO_2 was not observed until July. pCO_2 in April was 1831 ± 793 μatm, which was similar to 1805 ± 1010 μatm in January, and it increased 39.3 % to 2550 ± 1210 μatm in July. pCO_2 peaked in August (2885 ± 1351 μatm) and then decreased to 2176 ± 1166 in October. Overall, pCO_2 was 9.3 % and 21.7 % higher in wet season than in dry season for small and large rivers, respectively.

https://doi.org/10.5194/bg-2020-477
Preprint. Discussion started: 11 January 2021

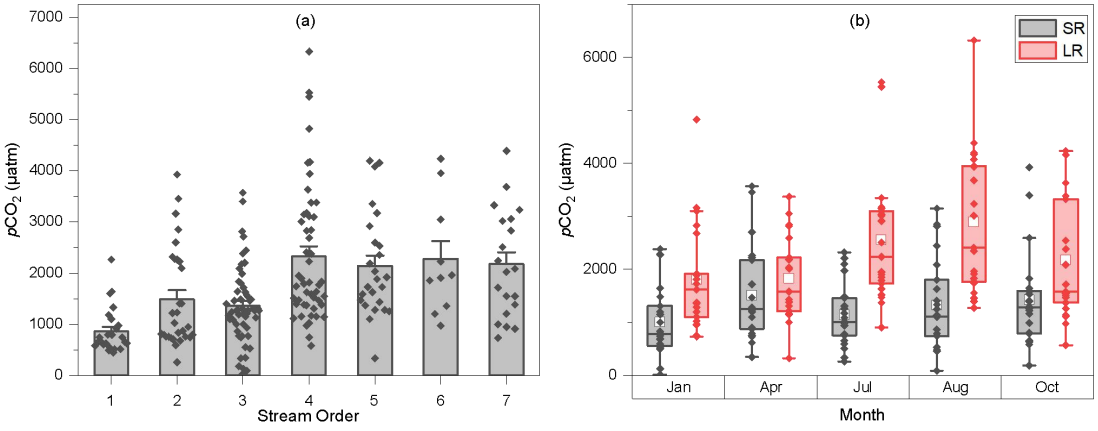

Figure 3 Spatial and Seasonal variations in pCO_2. (a) Yearly average pCO_2 in the seven stream orders, standard errors (SE) are displayed by error bars. (b) Seasonal pCO_2 in small and large rivers. The box mid-lines represent medians; the interquartile range (IQR) is represented by top and bottom of the box, respectively; whiskers indicate the range of 1.5 IQR; the white square symbols represent means, and the other symbols represent pCO_2 values for each sampled site.

3.3 CO_2 effluxes and k_{600}

CO_2 effluxes ranged from −129.8 to 3874.8 mmol m^{-2} d^{-1} with a mean of 225.2 mmol m^{-2} d^{-1}. More than 95 % of the 196 samples had positive FCO_2 values, indicating a carbon source. Overall, we observed higher FCO_2 during wet season than during dry season in both small and large rivers (Figure 4a). FCO_2 in small rivers and large rivers were 264.2 ± 410.0 and 300.1 ± 511.7 mmol m^{-2} d^{-1} respectively during the wet season, which was 87.2 % and 123.1 % higher compared to that in the dry season (141.1 ± 188.7 and 134.5 ± 129.5 mmol m^{-2} d^{-1} for small and large rivers respectively). No significant (independent sample t test, $p > 0.05$) difference in FCO_2 was observed between small and large rivers.

k_{600} differs greatly between river size classes and among hydrological periods (Figure 4b). k_{600} values in small rivers were significantly (independent sample t test, $p < 0.001$) higher on average than in large rivers. The mean values of k_{600} in small rivers were 8.29 ± 11.29 m d^{-1} and 4.90 ± 3.82 m d^{-1} for the wet season and dry season, respectively, which were 112.6 % and 70 % higher than that of large rivers (3.90 ± 5.55 m d^{-1} in the wet season and 2.25 ± 1.61 m d^{-1} in the dry season). k_{600} during the wet season were also significantly (independent sample t test, $p < 0.05$) higher than the dry season. k_{600} increased 112.7 % and 118.2 % from dry season to wet season in small and large rivers, respectively.

https://doi.org/10.5194/bg-2020-477
Preprint. Discussion started: 11 January 2021

However, comparisons between different phases in the same hydrological period did not differ significantly (paired sample t test, $p > 0.05$) for both river size classes.

The spatial and temporal variation of CO_2 efflux generally coincided with the changes in pCO_2 and k_{600} since high FCO_2 occurred when k_{600} or pCO_2 were elevated. In small rivers, the highest CO_2 effluxes were 346.8 ± 625.2 mmol m^{-2} d^{-1} during April, consistent with the high k_{600} and pCO_2 in this period. In large rivers, high CO_2 effluxes were observed in both April (339.9 ± 828.6 mmol m^{-2} d^{-1}) and August (3299.0 ± 270.0 mmol m^{-2} d^{-1}), which were attributed to high k_{600} in April and high pCO_2 in August.

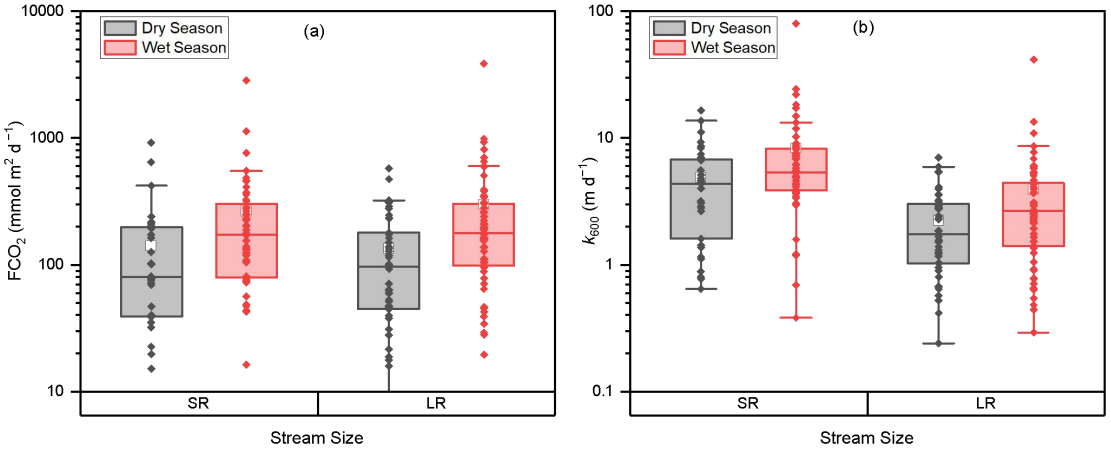

Figure 4 Relationship between stream size and (a) FCO_2 and (b) k_{600}. The box mid-lines represent medians; the interquartile range (IQR) is represented by top and bottom of the box, respectively; whiskers indicate the range of 1.5 IQR; the white square symbols represent means, and the other symbols represent FCO_2 and k_{600} values for each sampled site.

4 Discussions

4.1 Underlying Processes of pCO_2 dynamics

Previous studies show that riverine CO_2 originated from both lateral soil CO_2 input and in-stream metabolism (Yao et al., 2007; Li et al., 2013; Abril et al., 2014). The river water pCO_2 was positively related to DOC and negatively related to DO (Figure 5), indicating that decomposition of terrestrial organic carbon is an important source for pCO_2 (Stets et al., 2017; Liang et al., 2020). To compare the contribution of internal metabolism on pCO_2 in small and large rivers, ΔCO_2: ΔO_2 stoichiometry was used to evaluate the impact of respiration and photosynthesis processes on the concentration of O_2 and

https://doi.org/10.5194/bg-2020-477
Preprint. Discussion started: 11 January 2021

CO_2 in water bodies (Stets et al., 2017). The inverse relation between ΔCO_2 and ΔO_2 (Figure 6) demonstrated that metabolic processes are important for CO_2 variation (Amaral et al., 2020). However, the imbalanced ΔCO_2:ΔO_2 stoichiometry (Figure 6) indicates that, in addition to in-stream metabolic processes, other factors also affect the CO_2 and O_2 in the water (Stets et al., 2017). For example, 183 out of 215 observations are above the 1:1 ΔCO_2:ΔO_2 line, suggesting additional sources of carbon input. The difference in the ΔCO_2:ΔO_2 stoichiometry between small and large rivers reflects their differences in the controlling processes (Rasera et al., 2013). In large rivers, the ΔCO_2:ΔO_2 stoichiometry is closer to the 1:1 line than in small rivers, suggesting large rivers are more affected by the metabolic processes (Jeffrey et al., 2018; Amaral et al., 2020). In comparison, the deviation from the 1:1 line in small rivers indicates a stronger impact of additional carbon sources (Abril et al., 2014; Amaral et al., 2020).

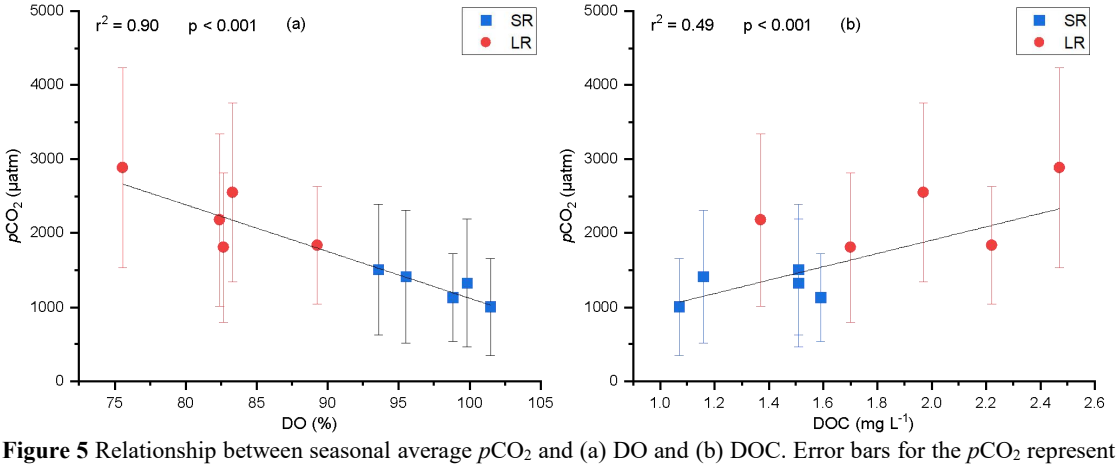

Figure 5 Relationship between seasonal average pCO_2 and (a) DO and (b) DOC. Error bars for the pCO_2 represent 1 standard deviation from the seasonal mean. The DO–pCO_2 and DOC–pCO_2 relationship are shown as solid lines.

https://doi.org/10.5194/bg-2020-477
Preprint. Discussion started: 11 January 2021

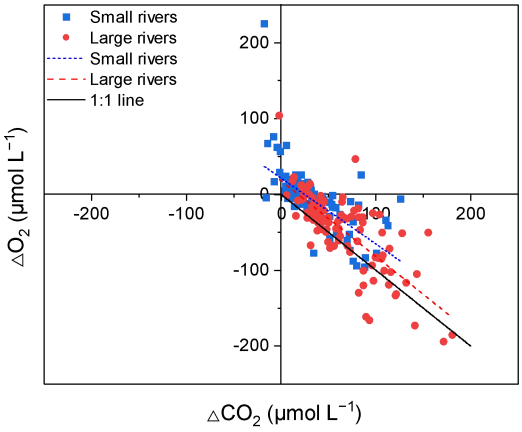

Figure 6 The relationship between ΔCO_2 and ΔO_2. Points greater than zero are oversaturated, and less than zero are undersaturated. Points above the 1:1 line would have extra carbon sources in addition to in-stream metabolic processes.

Differences in seasonal changes of pCO_2 between small and large rivers also suggest various primary controlling processes. pCO_2 in small rivers are mainly controlled by changes in lateral soil CO_2 input. The highest value of pCO_2 observed in April could be attributed to a rapid surge of additional soil CO_2 input caused by increasing precipitation (Figure 7). In spring, warming temperatures increase the net primary productivity of the terrestrial ecosystem, with a corresponding increase in soil carbon content. Meanwhile, increased precipitation in April facilitates the transportation of the soil carbon from land to the river system (Rasera et al., 2013). Thus, the temperature and precipitation in April dominantly control the soil CO_2 concentration, and hence mediate aqueous pCO_2 (Hope et al., 2004; Yao et al., 2007; Johnson et al., 2008). In contrast, a decrease of pCO_2 in July was observed, and it was likely the result of the CO_2 depletion effect in the soil combined with the dilution effect of precipitation. The soil carbon has experienced a depletion effect due to the continuous precipitation and soil erosion since April, limiting the supply of terrestrial carbon input for rivers in July (Hope et al., 2004; Johnson et al., 2007; Dinsmore et al., 2013). Meanwhile, the increase in precipitation and runoff can also cause a dilution effect, which leads to a decrease of pCO_2 (Ran et al., 2017b; Li et al., 2018). Seasonal variations in alkalinity substantiate the dilution effect and the depletion effect in July. Although the lowest alkalinity in small rivers was recorded in April, the highest pCO_2 values in small rivers were recorded in that month. It suggests that the effect of increased soil CO_2 input outweighs the dilution effects, both of which are caused by precipitation increase. In contrast, the synchronous upward trend

https://doi.org/10.5194/bg-2020-477
Preprint. Discussion started: 11 January 2021

315 of the alkalinity and pCO_2 in the later months of the year implies that the rise in pCO_2 results from weakened dilution effect (Ni et al., 2019). Moreover, low pCO_2 during dry season demonstrates inorganic carbon input via groundwater plays a minor role. Therefore, the variation of soil CO_2 input and dilution effect caused by precipitation are the main controlling factors of seasonal changes in riverine CO_2 among small rivers.

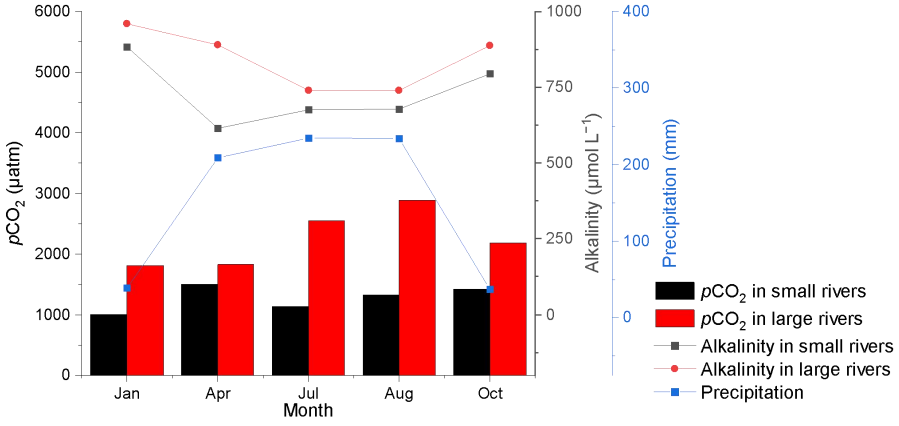

320

Figure 7 Seasonal variations of pCO_2, alkalinity, and precipitation.

On the other hand, high pCO_2 in large rivers is mainly a consequence of decomposition of organic carbon. Relatively low pCO_2 in April indicates a carbon source other than soil CO_2 input. When soil carbon dioxide enters river systems, it is readily emitted from the rivers into the air, with little reaching 325 the larger rivers downstream (Denfeld et al., 2013; Drake et al., 2018). The contribution of soil CO_2 input to pCO_2 could only be secondary. In large rivers, pCO_2 increased by 39.3 % from 1831 ± 793 μatm in April to 2550 ± 1210 μatm in July. The rise in temperature from April to July promoted a substantial increase in the net primary productivity of the terrestrial ecosystem and the content of terrestrial organic carbon entering the river (Borges et al., 2018). Yet, those terrestrial organic carbons 330 are difficult to convert into CO_2 in small rivers due to the high flow velocity and short water residence time (Hotchkiss et al., 2015). Thus, a possible explanation of increasing pCO_2 in large river is that a greater fraction of OC could be transported and fuel the heterotrophic respiration in large rivers, where long water residence time combined with the high temperature in July facilitate OC decomposition (Denfeld et al., 2013). For large rivers, recent studies have shown that the biological decomposition of

https://doi.org/10.5194/bg-2020-477
Preprint. Discussion started: 11 January 2021

allochthonous organic carbon caused by energetic microbial metabolism is the primary source of riverine CO_2 (Amaral et al., 2018; Jeffrey et al., 2018).

4.2 Environmental Control of k_{600} variation

Environmental factors, including wind speed and hydrological variables, could affect the gas exchange at the water–air interface and were typically used to explain the variance in k_{600} (Alin et al., 2011; Raymond et al., 2012). Flow velocity generally determine the k_{600} in rivers, while wind speed becomes a more important factor in controlling the k_{600} in large rivers, reservoirs and estuary (Guérin et al., 2007; Rasera et al., 2013; Amaral et al., 2020). In our surveyed rivers, k_{600} displayed a significant linear correlation (Pearson correlation, $p < 0.001$) with the flow velocity. Our k_{600} model (Figure 8) base on 188 field measurement data is similar to that developed by Alin et al. (2011) ($k_{600} = 13.82 + 0.35v$). However, in our studied rivers, no significant correlation (Pearson correlation， $p > 0.05$) was found between wind speed and k_{600} regardless of stream size. This could be explained by the lower wind speed (Table 2, 0.68 ± 0.66 m s^{-1} and 1.09 ± 1.06 m s^{-1} for small and large rivers, respectively) (Guérin et al., 2007). As the wind speed decreases, the impact of flow velocity on k_{600} will increase considerably (Borges et al., 2004). Therefore, the accuracy of k_{600} estimation based on wind speed in nearby regions should be examined using measurement data (Yao et al., 2007; Li et al., 2018). The temporal heterogeneities of k_{600} between small and large rivers reveal the differences in flow regime. k_{600} in small rivers are significantly (independent sample t test, $p < 0.001$) higher than in large rivers, which could be explained by higher flow velocity in small rivers due to a higher gradient. Meanwhile, significantly higher k_{600} (independent sample t test, $p < 0.05$) was also observed in the wet season compared to the dry season, which is the result of increasing flow velocity and turbulence due to plentiful monsoon-induced precipitation during wet season (Guérin et al., 2007; Alin et al., 2011; Ho et al., 2018).

https://doi.org/10.5194/bg-2020-477
Preprint. Discussion started: 11 January 2021

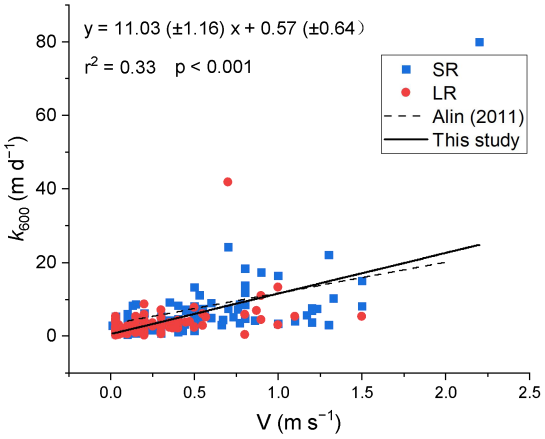

Figure 8 Relationship between k_{600} and flow velocity. The dashed line represents the parameterization of Alin et al (2011).

Table 2. Seasonal variation of k_{600} and environmental factors in small and large rivers.

Stream size	Season	Current velocity (m s^{-1})	U10 (m s^{-1})	k_{600} (m d^{-1})
small	Wet	0.66 ± 0.47	0.62 ± 0.61	8.29 ± 11.29
	Dry	0.43 ± 0.27	0.76 ± 0.73	4.90 ± 3.82
large	Wet	0.32 ± 0.32	0.86 ± 0.91	3.90 ± 5.55
	Dry	0.17 ± 0.19	1.43 ± 1.58	2.25 ± 1.61

Exceptionally high k_{600} values were observed in the surveyed rivers (Figure 8). The highest k_{600} in large and small rivers were 41.83 and 79.97 m d^{-1}, which were 5-fold and 3-fold larger than calculated k_{600}, respectively. This is the result of the exponential increase in k_{600} due to extreme flood events. Generally, flood events associated with heavy rainfall during the wet season can increase flow velocity and turbulence at the water–air interface (Almeida et al., 2017; Geeraert et al., 2017), leading to substantially higher k_{600}. Yet, neither our model nor the one from Alin et al. (2011) was suitable for the estimation of k_{600} during extreme flood events because the calculated k_{600} could deviate far from the measured k_{600} when they occurred. Therefore, the extent to which flood events affect k_{600} and riverine CO_2 emission is still uncertain and warrant continued research (Drake et al., 2018).

https://doi.org/10.5194/bg-2020-477
Preprint. Discussion started: 11 January 2021

4.3 A Comparison of CO_2 Emissions to Other Rivers

The mean CO_2 fluxes of 225.2 mmol m^{-2} d^{-1} in DJRB is comparable to those observed in tropical and subtropical rivers in the Americas, Africa, and Southeast Asia (Table 3). Although the magnitude of the CO_2 evasion of these river basins is similar, the seasonal variations and drivers behind them could differ. The higher CO_2 emission in the Dongjiang Basin was observed in the wet season compared to the dry season, and this seasonal pattern is similar to that observed in the Xijiang and Daning rivers (Yao et al., 2007; Ni et al., 2019) but different from the one from Jinshui River in the upper reaches of the Yangtze River, where pCO_2 is high in winter and low in summer (Luo et al., 2019), even though all four rivers are in the East Asia Monsoon climate region. The difference in seasonal pattern can be explained by the drivers of pCO_2 variability as the seasonal variation of riverine pCO_2 is the result of the increase of CO_2 input and the dilution effect caused by precipitation (Johnson et al., 2007). For rivers where pCO_2 is lower in summer than in winter, the dilution effect overrides the effect of increased carbon input. In contrast, for rivers like the Dongjiang river, although the dilution effect remains, increased CO_2 input and metabolism are more significant factors in controlling pCO_2, thus leading to higher summer pCO_2. In addition, the controlling processes of the Dongjiang River may be different even when compared to rivers with similar seasonal variations in the same climatic zone. For instance, DO in the Xijiang river was supersaturated, indicating that photosynthetic activities in the water body mainly reduce the CO_2 concentration in the rivers (Yao et al., 2007). Therefore, other carbon sources like soil respiration and carbonate weathering should be responsible for high pCO_2 in summer (Zhang et al., 2019). In contrast, low DO value and a negative correlation between DO and pCO_2 have been observed in the Dongjiang River, indicating that the respiration in the water body is an essential source of riverine CO_2 (Stets et al., 2017) and results in higher pCO_2 in summer.

The CO_2 fluxes in small rivers are similar to that in large rivers, which is contradictory to the finding in previous studies that CO_2 effluxes should be higher in small rivers compared to large rivers due to the input of CO_2-rich groundwater (Duvert et al., 2018). The depletion and diffusion effect may be responsible for the discrepancy (Johnson et al., 2007; Dinsmore et al., 2013). In the Dongjiang River Basin, groundwater could be easily diluted due to ample monsoon-induced precipitation, preventing it from supplying the small rivers with high concentrations of carbon dioxide. However, we recognize that the impact of groundwater on pCO_2 in small rivers may be overlooked in our sampling process since the CO_2 carried by groundwater can emit into the atmosphere within a very short distance (Duvert

https://doi.org/10.5194/bg-2020-477
Preprint. Discussion started: 11 January 2021

et al., 2018). In view of the above, it is recommended that further studies targeting the release of groundwater CO_2 to the atmosphere be carried out in the future.

Table 3. Comparison of CO_2 emission in subtropical and tropical rivers.

Rivers	Climate	Season	pCO_2 (μatm)	k_{600} (m d^{-1})	FCO_2 (mmol m^{-2} d^{-1})	References
The Dongjiang River (Large rivers)	Subtropical	Wet	2422 ± 1209	3.90 ± 5.55	300.1 ± 511.8	This study
		Dry	1990 ± 1094	2.25 ± 1.61	134.5 ± 129.5	
The Dongjiang River (small rivers)		Wet	1321 ± 792	8.29 ± 11.29	264.2 ± 410.0	
		Dry	1191 ± 825	4.90 ± 3.82	129.5 ± 197.2	
The Xijiang River (Mainstream)	Subtropical		2600		190.3–358.6	(Yao et al., 2007)
The Lower Meikong River	Tropical		1090 ± 290	6.24*	194.5	(Li et al., 2013)
The Yangtze River (Jinshui River) (headwater stream)	Subtropical		1147 ± 874	11.1 ± 4.5*	343 ± 413	(Luo et al., 2019)
		Dry	1562 ± 975		542 ± 477	
		Wet	834 ± 639		192 ± 278	
The upper Yangtze River (Daning river)	Subtropical		1198.2 ± 1122.9		329.8 ± 470.2	(Ni et al., 2019)
		Rainy	1243.7 ± 1111.5	8.1–14.1*	357.4 ± 483.7	
		Dry	1145.5 ± 1146.2	7.0–8.8*	288.7 ± 450.0	
The Zambezi River	Tropical	Wet	3102.5 ppm	0.05–1.51	350.75	(Teodoru et al., 2014)
		Dry	1150 ppm		51.92	
The Lower Red River	Tropical		1589 ± 43	12.22 ± 6.48	530.3 ± 16.9	(Le et al., 2018)
Caboolture River	Subtropical		3000 ± 33		379 ± 53	(Jeffrey et al., 2018)
Rajang River	Tropical	wet	2531 ± 188	0.55–2.93	141.67	(Müller-Dum et al., 2019)
		dry	2337 ± 304		125	
Mississippi River	Subtropical		1514 ± 652		172.8	(Reiman and Xu, 2019)
Amazonian Rivers	Tropical		259–7808	5.06	69.12–1321.92	(Rasera et al., 2013)

405 * k values have been showed here because k_{600} values were not provided in references

https://doi.org/10.5194/bg-2020-477
Preprint. Discussion started: 11 January 2021

5 Conclusion

Studying CO_2 emissions from subtropical rivers is an essential step toward more accurate estimates of global CO_2 evasion from river systems. By deploying floating chambers, seasonal changes in riverine pCO_2 and CO_2 evasion in the Dongjiang river catchment were investigated. Lateral soil CO_2 input and dilution effect caused by precipitation played critical roles in controlling riverine pCO_2 in small rivers, while the decomposition of allochthonous organic carbon is responsible for pCO_2 changes in large rivers as suggested by the ΔCO_2: ΔO_2 stoichiometry line. k_{600} was higher in small rivers than large rivers and higher during the wet season than the dry season, both of which can be explained by the observed significant correlation between k_{600} and the flow velocity. In contrast to previous studies, similar CO_2 fluxes were observed among small and large rivers in the DJRB. It is suggested that the absence of commonly observed higher CO_2 fluxes in small rivers could be associated with the depletion effect caused by abundant and persistent precipitation in this subtropical monsoon catchment. There is no doubt that the spatial and temporal variation of CO_2 evasion in the DJRB reflected the complexity and diversity of controlling factors. As a step towards a more accurate estimate of the carbon budget in the catchment, comprehensive and systematic measurements of CO_2 evasion covering a broad range of stream sizes and seasons are of paramount importance.

Data availability. CO_2 emission data used in this study are available online at: https://doi.org/10.25442/hku.13416281.v1 (Liu, 2020). Other data are available from the corresponding author Lishan Ran upon request at lsran@hku.hk.

Author contributions. BL and LR designed field sampling. BL, MT, CC, XY, and LR carried out the fieldwork. BL, MT, and KS designed and performed the laboratory analysis. BL composed the manuscript with contributions from all authors.

Competing interests. The authors declare that they have no conflict of interest.

Acknowledgements. This work was financially supported by the Research Grants Council of Hong Kong (Grants: 17300619 and 27300118) and the National Natural Science Foundation of China (Grant: 41807318).

https://doi.org/10.5194/bg-2020-477
Preprint. Discussion started: 11 January 2021

References

Abril, G., Martinez, J. M., Artigas, L. F., Moreira-Turcq, P., Benedetti, M. F., Vidal, L., Meziane, T., Kim, J. H., Bernardes, M. C., Savoye, N., Deborde, J., Souza, E. L., Alberic, P., Landim de Souza, M. F., and Roland, F.: Amazon River carbon dioxide outgassing fuelled by wetlands, Nature, 505, 395-398, https://doi.org/10.1038/nature12797, 2014.

Abril, G., Bouillon, S., Darchambeau, F., Teodoru, C. R., Marwick, T. R., Tamooh, F., Ochieng Omengo, F., Geeraert, N., Deirmendjian, L., Polsenaere, P., and Borges, A. V.: Technical Note: Large overestimation of pCO_2 calculated from pH and alkalinity in acidic, organic-rich freshwaters, Biogeosciences, 12, 67-78, https://doi.org/10.5194/bg-12-67-201510.5194, 2015.

Alin, S. R., Rasera, M. d. F. F. L., Salimon, C. I., Richey, J. E., Holtgrieve, G. W., Krusche, A. V., and Snidvongs, A.: Physical controls on carbon dioxide transfer velocity and flux in low-gradient river systems and implications for regional carbon budgets, Journal of Geophysical Research, 116, G01009, https://doi.org/10.1029/2010jg001398, 2011.

Almeida, R. M., Pacheco, F. S., Barros, N., Rosi, E., and Roland, F.: Extreme floods increase CO_2 outgassing from a large Amazonian river, Limnology and Oceanography, 62, 989-999, https://doi.org/10.1002/lno.10480, 2017.

Amaral, J. H. F., Borges, A. V., Melack, J. M., Sarmento, H., Barbosa, P. M., Kasper, D., de Melo, M. L., De Fex-Wolf, D., da Silva, J. S., and Forsberg, B. R. J. S. o. t. T. E.: Influence of plankton metabolism and mixing depth on CO_2 dynamics in an Amazon floodplain lake, Science of the Total Environment, 630, 1381-1393, https://doi.org/10.1016/j.scitotenv.2018.02.331, 2018.

Amaral, J. H. F., Melack, J. M., Barbosa, P. M., MacIntyre, S., Kasper, D., Cortés, A., Silva, T. S. F., Nunes de Sousa, R., and Forsberg, B. R.: Carbon dioxide fluxes to the atmosphere from waters within flooded forests in the Amazon basin, Journal of Geophysical Research: Biogeosciences, 125, e2019JG005293, https://doi.org/10.1029/2019JG005293, 2020.

Battin, T. J., Luyssaert, S., Kaplan, L. A., Aufdenkampe, A. K., Richter, A., and Tranvik, L. J.: The boundless carbon cycle, Nature Geoscience, 2, 598-600, https://doi.org/10.1038/ngeo618, 2009.

Borges, A. V., Delille, B., Schiettecatte, L. S., Gazeau, F., Abril, G., Frankignoulle, M. J. L., and Oceanography: Gas transfer velocities of CO_2 in three European estuaries (Randers Fjord, Scheldt, and Thames), Limnology Oceanography, 49, 1630-1641, https://doi.org/10.4319/lo.2004.49.5.1630, 2004.

Borges, A. V., Darchambeau, F., Lambert, T., Bouillon, S., Morana, C., Brouyere, S., Hakoun, V., Jurado, A., Tseng, H. C., Descy, J. P., and Roland, F. A. E.: Effects of agricultural land use on fluvial carbon dioxide, methane and nitrous oxide concentrations in a large European river, the Meuse (Belgium), Science of The Total Environment, 610-611, 342-355, https://doi.org/10.1016/j.scitotenv.2017.08.047, 2018.

Chen, Y. D., Zhang, Q., Lu, X., Zhang, S., and Zhang, Z.: Precipitation variability (1956–2002) in the Dongjiang River (Zhujiang River basin, China) and associated large-scale circulation, Quaternary International, 244, 130-137, https://doi.org/10.1016/j.quaint.2010.08.013, 2011.

Cole, J. J., Prairie, Y. T., Caraco, N. F., McDowell, W. H., Tranvik, L. J., Striegl, R. G., Duarte, C. M., Kortelainen, P., Downing, J. A., Middelburg, J. J., and Melack, J.: Plumbing the global carbon cycle: Integrating inland waters into the terrestrial carbon budget, Ecosystems, 10, 172-185, https://doi.org/10.1007/s10021-006-9013-8, 2007.

Denfeld, B. A., Frey, K. E., Sobczak, W. V., Mann, P. J., and Holmes, R. M.: Summer CO_2 evasion from streams and rivers in the Kolyma River basin, north-east Siberia, Polar Research, 32, 19704,

https://doi.org/10.5194/bg-2020-477
Preprint. Discussion started: 11 January 2021

https://doi.org/10.3402/polar.v32i0.19704, 2013.
Dickson, A. G., Sabine, C. L., and Christian, J. R.: Guide to best practices for ocean CO_2 measurements, North Pacific Marine Science Organization, 2007.
Ding, J., Jiang, Y., Fu, L., Liu, Q., Peng, Q., and Kang, M.: Impacts of land use on surface water quality in a subtropical river basin: A case study of the Dongjiang River Basin, Southeastern China, Water, 7, 4427-4445, https://doi.org/10.3390/w7084427, 2015.
Dinsmore, K. J., Wallin, M. B., Johnson, M. S., Billett, M. F., Bishop, K., Pumpanen, J., and Ojala, A.: Contrasting CO_2 concentration discharge dynamics in headwater streams: A multi-catchment comparison, Journal of Geophysical Research: Biogeosciences, 118, 445-461, https://doi.org/10.1002/jgrg.20047, 2013.
Drake, T. W., Raymond, P. A., and Spencer, R. G.: Terrestrial carbon inputs to inland waters: A current synthesis of estimates and uncertainty, Limnology and Oceanography Letters, 3, 132-142, https://doi.org/10.1002/lol2.10055, 2018.
Duvert, C., Butman, D. E., Marx, A., Ribolzi, O., and Hutley, L. B.: CO_2 evasion along streams driven by groundwater inputs and geomorphic controls, Nature Geoscience, 11, 813-818, https://doi.org/10.1038/s41561-018-0245-y, 2018.
Fu, Y., Tang, C., Li, J., Zhao, Y., Zhong, W., and Zeng, X.: Sources and transport of organic carbon from the Dongjiang River to the Humen outlet of the Pearl River, southern China, Journal of Geographical Sciences, 24, 143-158, https://doi.org/10.1007/s11442-014-1078-2, 2014.
Geeraert, N., Omengo, F. O., Borges, A. V., Govers, G., and Bouillon, S.: Shifts in the carbon dynamics in a tropical lowland river system (Tana River, Kenya) during flooded and non-flooded conditions, Biogeochemistry, 132, 141-163, https://doi.org/10.1007/s10533-017-0292-2, 2017.
Guérin, F., Abril, G., Serça, D., Delon, C., Richard, S., Delmas, R., Tremblay, A., and Varfalvy, L.: Gas transfer velocities of CO_2 and CH_4 in a tropical reservoir and its river downstream, Journal of Marine Systems, 66, 161-172, https://doi.org/10.1016/j.jmarsys.2006.03.019, 2007.
Ho, D. T., Engel, V. C., Ferrón, S., Hickman, B., Choi, J., and Harvey, J. W.: On factors influencing air - water gas exchange in emergent wetlands, Journal of Geophysical Research: Biogeosciences, 123, 178-192, https://doi.org/10.1002/2017JG004299, 2018.
Hope, D., Palmer, S. M., Billett, M. F., and Dawson, J. J. J. H. P.: Variations in dissolved CO_2 and CH_4 in a first - order stream and catchment: an investigation of soil–stream linkages, Journal of Hydrological Processes, 18, 3255-3275, https://doi.org/10.1002/hyp.5657, 2004.
Hotchkiss, E., Hall Jr, R., Sponseller, R., Butman, D., Klaminder, J., Laudon, H., Rosvall, M., and Karlsson, J. J. N. G.: Sources of and processes controlling CO_2 emissions change with the size of streams and rivers, Nature Geoscience, 8, 696-699, https://doi.org/10.1038/ngeo2507, 2015.
Jeffrey, L. C., Santos, I. R., Tait, D. R., Makings, U., and Maher, D. T.: Seasonal drivers of carbon dioxide dynamics in a hydrologically modified subtropical tidal river and estuary (Caboolture River, Australia), Journal of Geophysical Research: Biogeosciences, 123, 1827-1849, https://doi.org/10.1029/2017jg004023, 2018.
Johnson, M. S., Weiler, M., Couto, E. G., Riha, S. J., and Lehmann, J.: Storm pulses of dissolved CO_2 in a forested headwater Amazonian stream explored using hydrograph separation, Water resources research, 43, https://doi.org/10.1029/2007WR006359, 2007.
Johnson, M. S., Lehmann, J., Riha, S. J., Krusche, A. V., Richey, J. E., Ometto, J. P. H., and Couto, E. G.: CO_2 efflux from Amazonian headwater streams represents a significant fate for deep soil respiration, Geophysical Research Letters, 35, https://doi.org/10.1029/2008GL034619, 2008.
Lauerwald, R., Laruelle, G. G., Hartmann, J., Ciais, P., and Regnier, P. A.: Spatial patterns in CO_2 evasion from the global river network, Global Biogeochemical Cycles, 29, 534-554,

https://doi.org/10.1002/2014GB004941, 2015.

Le, T. P. Q., Marchand, C., Ho, C. T., Da Le, N., Duong, T. T., Lu, X., Doan, P. K., Nguyen, T. K., Nguyen, T. M. H., and Vu, D. A.: CO_2 partial pressure and CO_2 emission along the lower Red River (Vietnam), Biogeosciences, 15, 4799-4814, https://doi.org/10.5194/bg-15-4799-2018, 2018.

Li, S., Lu, X. X., and Bush, R. T.: CO_2 partial pressure and CO_2 emission in the Lower Mekong River, Journal of Hydrology, 504, 40-56, https://doi.org/10.1016/j.jhydrol.2013.09.024, 2013.

Li, S., Ni, M., Mao, R., and Bush, R. T.: Riverine CO_2 supersaturation and outgassing in a subtropical monsoonal mountainous area (Three Gorges Reservoir Region) of China, Journal of Hydrology, 558, 460-469, https://doi.org/10.1016/j.jhydrol.2018.01.057, 2018.

Liang, B., Hu, J. T., Li, S. Y., Ye, Y. X., Liu, D. H., and Huang, J.: Carbon system simulation in the Pearl River Estuary, China: Mass fluxes and transformations, Journal of Geophysical Research: Biogeosciences, 125, e2019JG005012, https://doi.org/10.1029/2019jg005012, 2020.

Liu, Boyi.: Riverine CO_2 Emission Datasets: Dongjiang River. The University of Hong Kong. Dataset. https://doi.org/10.25442/hku.13416281.v1, 2020.

Luo, J., Li, S., Ni, M., and Zhang, J.: Large spatiotemporal shifts of CO_2 partial pressure and CO_2 degassing in a monsoonal headwater stream, Journal of Hydrology, 579, 124135, https://doi.org/10.1016/j.jhydrol.2019.124135, 2019.

Marx, A., Dusek, J., Jankovec, J., Sanda, M., Vogel, T., van Geldern, R., Hartmann, J., and Barth, J. A. C.: A review of CO_2 and associated carbon dynamics in headwater streams: A global perspective, Reviews of Geophysics, 55, 560-585, https://doi.org/10.1002/2016rg000547, 2017.

Millero, F. J., Graham, T. B., Huang, F., Bustos-Serrano, H., and Pierrot, D.: Dissociation constants of carbonic acid in seawater as a function of salinity and temperature, Marine Chemistry, 100, 80-94, https://doi.org/10.1016/j.marchem.2005.12.001, 2006.

Müller-Dum, D., Warneke, T., Rixen, T., Müller, M., Baum, A., Christodoulou, A., Oakes, J., Eyre, B. D., and Notholt, J.: Impact of peatlands on carbon dioxide (CO_2) emissions from the Rajang River and Estuary, Malaysia, Biogeosciences, 16, 17-32, https://doi.org/10.5194/bg-16-17-2019., 2019.

Ni, M., Li, S., Luo, J., and Lu, X.: CO_2 partial pressure and CO_2 degassing in the Daning River of the upper Yangtze River, China, Journal of Hydrology, 569, 483-494, https://doi.org/10.1016/j.jhydrol.2018.12.017, 2019.

Ran, L., Lu, X. X., Yang, H., Li, L., Yu, R., Sun, H., and Han, J.: CO_2 outgassing from the Yellow River network and its implications for riverine carbon cycle, Journal of Geophysical Research: Biogeosciences, 120, 1334-1347, https://doi.org/10.1002/2015jg002982, 2015.

Ran, L., Li, L., Tian, M., Yang, X., Yu, R., Zhao, J., Wang, L., and Lu, X.: Riverine CO_2 emissions in the Wuding River catchment on the Loess Plateau: Environmental controls and dam impoundment impact, Journal of Geophysical Research: Biogeosciences, 122, 1439-1455, https://doi.org/10.1002/2016JG003713, 2017a.

Ran, L., Lu, X. X., and Liu, S.: Dynamics of riverine CO_2 in the Yangtze River fluvial network and their implications for carbon evasion, Biogeosciences, 14, 2183-2198, https://doi.org/10.5194/bg-14-2183-2017, 2017b.

Rasera, M. d. F. F., Krusche, A. V., Richey, J. E., Ballester, M. V., and Victoria, R. L.: Spatial and temporal variability of pCO_2 and CO_2 efflux in seven Amazonian Rivers, Biogeochemistry, 116, 241-259, https://doi.org/10.1007/s10533-013-9854-0, 2013.

Raymond, P. A., Zappa, C. J., Butman, D., Bott, T. L., Potter, J., Mulholland, P., Laursen, A. E., McDowell, W. H., and Newbold, D.: Scaling the gas transfer velocity and hydraulic geometry in streams and small rivers, Limnology and Oceanography: Fluids and Environments, 2, 41-53, https://doi.org/10.1215/21573689-1597669, 2012.

https://doi.org/10.5194/bg-2020-477
Preprint. Discussion started: 11 January 2021

Raymond, P. A., Hartmann, J., Lauerwald, R., Sobek, S., McDonald, C., Hoover, M., Butman, D., Striegl, R., Mayorga, E., and Humborg, C.: Global carbon dioxide emissions from inland waters, Nature, 503, 355-359, https://doi.org/10.1038/nature12760, 2013.

Reiman, J. H., and Xu, Y. J.: Dissolved carbon export and CO_2 outgassing from the lower Mississippi River – Implications of future river carbon fluxes, Journal of Hydrology, 578, 124093, https://doi.org/10.1016/j.jhydrol.2019.124093, 2019.

Sawakuchi, H. O., Neu, V., Ward, N. D., Barros, M. d. L. C., Valerio, A. M., Gagne-Maynard, W., Cunha, A. C., Less, D. F. S., Diniz, J. E. M., Brito, D. C., Krusche, A. V., and Richey, J. E.: Carbon dioxide emissions along the lower Amazon River, Frontiers in Marine Science, 4, https://doi.org/10.3389/fmars.2017.00076, 2017.

Stets, E. G., Butman, D., McDonald, C. P., Stackpoole, S. M., DeGrandpre, M. D., and Striegl, R. G.: Carbonate buffering and metabolic controls on carbon dioxide in rivers, Global Biogeochemical Cycles, 31, 663-677, https://doi.org/10.1002/2016gb005578, 2017.

Tao, Z., Gao, Q., Wang, Z., Zhang, S., Xie, C., Lin, P., Ruan, X., Li, S., and Mao, H.: Estimation of carbon sinks in chemical weathering in a humid subtropical mountainous basin, Chinese Science Bulletin, 56, 3774-3782, https://doi.org/10.1007/s11434-010-4318-6, 2011.

Teodoru, C., Nyoni, F., Borges, A., Darchambeau, F., Nyambe, I., and Bouillon, S.: Spatial variability and temporal dynamics of greenhouse gas (CO_2, CH_4, N_2O) concentrations and fluxes along the Zambezi River mainstem and major tributaries, Biogeosciences Discussion, 11, 16391-16445, https://doi.org/10.5194/bgd-11-16391-2014, 2014.

Tian, M., Yang, X., Ran, L., Su, Y., Li, L., Yu, R., Hu, H., and Lu, X. X.: Impact of land cover types on riverine CO_2 outgassing in the Yellow River source region, Water, 11, 2243, https://doi.org/10.3390/w11112243, 2019.

Wanninkhof, R.: Relationship between wind speed and gas exchange over the ocean, Journal of Geophysical Research: Oceans, 97, 7373-7382, https://doi.org/10.1029/92JC00188, 1992.

Weiss, R. F.: Carbon dioxide in water and seawater: the solubility of a non-ideal gas, Marine Chemistry, 2, 203-215, https://doi.org/10.1016/0304-4203(74)90015-2, 1974.

Yao, G., Gao, Q., Wang, Z., Huang, X., He, T., Zhang, Y., Jiao, S., and Ding, J.: Dynamics of CO_2 partial pressure and CO_2 outgassing in the lower reaches of the Xijiang River, a subtropical monsoon river in China, Science of The Total Environment, 376, 255-266, https://doi.org/10.1016/j.scitotenv.2007.01.080, 2007.

Zhang, L., Qin, X., Liu, P., Huang, Q., Lan, F., and Ji, H.: Estimation of carbon sink fluxes in the Pearl River basin (China) based on a water–rock–gas–organism interaction model, Environmental Earth Sciences, 74, 945-952, https://doi.org/10.1007/s12665-014-3788-2, 2015.

Zhang, S., Lu, X. X., Higgitt, D. L., Chen, C.-T. A., Han, J., and Sun, H.: Recent changes of water discharge and sediment load in the Zhujiang (Pearl River) Basin, China, Global and Planetary Change, 60, 365-380, https://doi.org/10.1016/j.gloplacha.2007.04.003, 2008.

Zhang, T., Li, J., Pu, J., and Yuan, D.: Carbon dioxide exchanges and their controlling factors in Guijiang River, SW China, Journal of Hydrology, 578, 124073, https://doi.org/10.1016/j.jhydrol.2019.124073, 2019.